



The three-dimensional microfabric of turbidite sequences: Insights into sedimentary processes within the Miocene arc-arc junction in central Hokkaido

メタデータ	言語: eng 出版者: 公開日: 2022-02-10 キーワード (Ja): キーワード (En): 作成者: Itoh, Yasuto, Tamaki, Machiko, 伊藤, 康人 メールアドレス: 所属:
URL	http://hdl.handle.net/10466/00016749

In: Horizons in Earth Science Research... ISBN: 978-1-53619-835-5
Editors: B. Veress and J. Szigethy © 2021 Nova Science Publishers, Inc.

Chapter 4

**THE THREE-DIMENSIONAL MICROFABRIC
OF TURBIDITE SEQUENCES:
INSIGHTS INTO SEDIMENTARY PROCESSES
WITHIN THE MIOCENE ARC-ARC JUNCTION
IN CENTRAL HOKKAIDO**

Yasuto Itoh^{1,} and Machiko Tamaki²*

¹Osaka Prefecture University, Sakai, Osaka, Japan

²Japan Oil Engineering Co., Ltd., Tokyo, Japan

ABSTRACT

Central Hokkaido, which is situated on the northwestern Pacific margin, has been the site of significant development of foreland basins in conjunction with a strong transpressive regime resulting from an arc-arc collision since the Neogene. The burial and exhumation processes occurring in voluminous basin fills can help to elucidate the dynamic material recycling mechanisms that occur at convergent plate margins. In

* Corresponding Author's E-mail: yasutokov@yahoo.co.jp.

the present work, the microfabric of the Kawabata Formation (a sequence of thick turbidites and associated coarse clastics in the middle Miocene) was quantitatively assessed by evaluating rock specimens using magnetic techniques. The anisotropy of magnetic susceptibility (AMS) was used to study sedimentary structures, and the paleocurrent directions of these Kawabata samples were determined based on finding the principal AMS axes. After correcting for tectonic block rotation, the majority of the samples demonstrated a preferential westward sediment influx with a minor contribution of a southward component. This result was in agreement with the burial process of the N-S elongate foreland basin accompanied by the eastern hinterland at the collision front. A re-deposition experiment involving fine detrital grains indicated that the AMS fabric of the Miocene turbidites was primarily governed by the linear or planar alignment of paramagnetic minerals having significant shape anisotropy. In addition to the conventional AMS analyses, a unique method for the visualization of anisotropic rock fabrics was employed to reconstruct the prevailing azimuths of the fluid flow in pores. The magnetic anisotropy was monitored for the samples impregnated with a solvent containing a suspension of a magnetic powder (that is, a ferrofluid). This process successfully delineated fracture networks that had developed within the tight sandstone in the Kawabata Formation. Rock specimens assessed using the ferrofluid showed significantly different AMS patterns from raw samples taken from the same horizon, and this difference is believed to reflect the tectonic control of rupture propagation in response to intense tectonic stress in the collision front around central Hokkaido. Micro-focus three-dimensional density images of test pieces were obtained utilizing an X-ray computerized tomography scanner, and depicted inhomogeneous impregnation of the ferrofluid as a result of small-scale structural disturbances within the rocks. Variations in impregnation efficiency between samples are likely the result of bioturbation, which affects the movement of the dense fluid through sinuous pathways. Using the latest technology of digital image processing, both trace fossils and fragments of tube worms were identified. This work shows that magnetic analysis has the potential to elucidate evolutionary processes in sedimentary basins in Hokkaido on the basis of microbial activity. This technique is evidently a versatile methodology with applications in multidisciplinary research studying the interactions between the planet and living organisms, and could be used to study other active margins worldwide.

1. INTRODUCTION

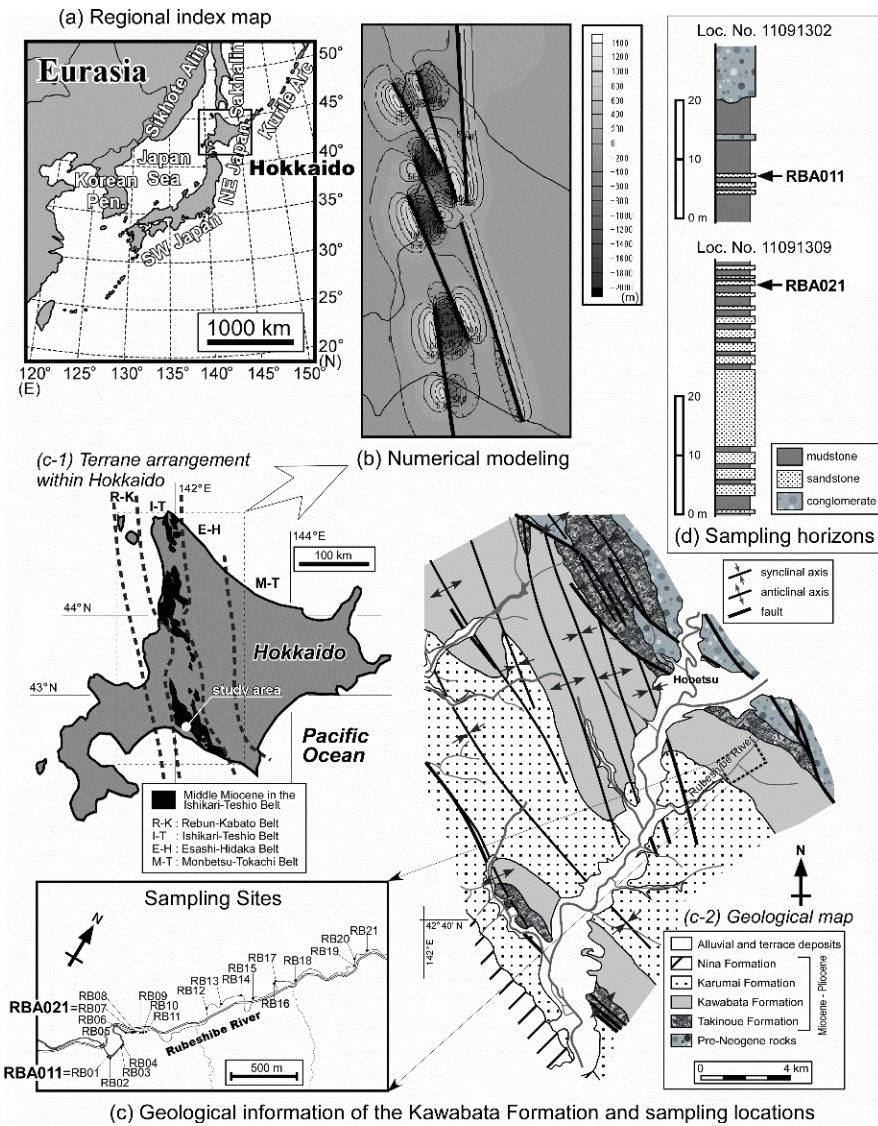


Figure 1. The geological and geophysical characteristics of the study area. (a) A regional index map. (b) A dislocation model of the Miocene basins in central Hokkaido (modified from Itoh et al., 2014a). (c) Miocene geological information for the area surrounding the Kawabata Formation and sampling locations along the Rubeshibe River. (d) Sampling horizons on columnar sections.

Hokkaido is an island comprising a part of northern Japan and located at the junction of the Kurile and northeast Japan arcs (Figure 1a). As a result of the effect of the prolonged oblique collision of the arcs on the northwestern Pacific convergent margin, both mountain and basin formation proceeded in central Hokkaido throughout the late Cenozoic (Itoh et al., 2014a). Basin-filling sediments in this region show the exhumation of the deformation front during successive tectonic events, such as the amalgamation of crustal blocks on a closing marginal sea plate (ca. 30 Ma; Itoh et al., 2017) and the spreading of the Japan Sea backarc basin (ca. 20~15 Ma; Otofujii et al., 1994).

In an effort to obtain quantitative data regarding the tectono-sedimentological properties of the tectonic basins, the authors performed a number of magnetic studies of rocks over the past decade (Itoh et al., 2013, 2014b, 2016). This research confirmed that the anisotropy of magnetic susceptibility (AMS) in sedimentary rocks reflects the microscopic fabrics that originate from the alignment of detrital grains and/or the preferred azimuth of fractures formed during orogenic movements. The present paper represents a comprehensive review of a series of such rock magnetic studies. The emphasis is on the AMS analysis of samples impregnated with a solvent in which an ultrafine magnetic powder has been suspended (hereafter referred to as a ferrofluid) as a means of delineating the three-dimensional architectures of fracture networks developed under tectonic stresses. The ferrofluid-soaked rocks examined in this work provide AMS data that are correlated with the anisotropy of liquid permeability and also enable the observation of intact benthic organisms after digital imaging of computerized tomography (CT) data. High-resolution original images of microfossils preserved within the Miocene turbidite sequence resulting from this technique are also presented herein.

2. BACKGROUND

The arc-arc oblique (right lateral) collision event in the vicinity of central Hokkaido peaked during the Miocene period and resulted in the

development of a west-vergent fold-thrust zone and an elongate foreland depression (as long as 400 km) within the Ishikari-Teshio Belt (Figure 1c-1). Kawakami (2013) divided the tectonic sag into the Tenpoku, Haboro, Ishikari and Hidaka basins, going from north to south. The Ishikari basin was filled with lower basinal turbidites and upper slope-apron turbidites in the mid-to-late Miocene Kawabata Formation, which is 3500 m thick. Kawakami proposed that the tightly grouped paleocurrent data acquired from the sedimentary unit parallel to the N-S basin axis indicates that the incipient depression has a confined floor, the western side of which is cut by the Umaoi active fault.

Kawakami et al. (1999) studied the Kawabata Formation in the Hobetsu region located in the southern part of the Ishikari-Teshio Belt, and reported that this region is characterized by monotonous alternations of sandstone and mudstone that are intercalated with sheet-like coarse clastics derived from the eastern hinterland. A sedimentological investigation by the same group established that metamorphic zones in the Esashi-Hidaka Belt (Figure 1c-1) are the most significant provenance. In this study, the authors employed a sampling route that ran along the Rubeshibe River (Figure 1c-2), where the Kawabata sequence is highly exposed with only minor structural disturbance.

As shown in Figure 1c, samples of the Kawabata Formation were taken at 21 sites (representing the RB-series) along the Rubeshibe River route (Itoh et al., 2013) using a battery-powered electric drill, and cores 25 mm in diameter were independently oriented using a magnetic compass. The bedding attitudes were recorded at each location to allow correction for tectonic tilting. Cylindrical specimens 22 mm in length were subsequently cut from the cores in the laboratory. Additional sampling for the ferrofluid experiments was later performed by Itoh et al. (2014b). At that time, oriented hand samples were collected from two outcrops: RBA011 (the same site as the RB01 location sampled by Itoh et al. in 2013, comprising a muddy channel and levee turbidite) and RBA021 (the same site as the RB07 location sampled by Itoh et al. in 2013, comprising sandy sheet turbidite), as indicated in Figure 1c. These samples were obtained from sandy parts of the exposed sections (Figure 1d), whereas the

paleomagnetic samples of Itoh et al. (2013) tended to be muddy, since fine-grained sediments generally preserve stable remanent magnetization.

Low-field bulk magnetic susceptibility data were acquired for all specimens using a Bartington MS2 susceptibility meter, following which the natural remanent magnetizations (NRMs) of the samples were determined with a cryogenic magnetometer (model 760-R SRM, 2-G Enterprises) in a magnetically shielded room at Kyoto University.

3. METHODOLOGY

3.1. Demagnetization Tests

To isolate stable components of the remanent magnetization, representative specimens from each RB-site, which exhibited average NRM directions, were subjected to progressive alternating field demagnetization (PAFD) and progressive thermal demagnetization (PThD). PAFD was performed up to 80 mT in a μ -metal envelope using a three-axis sample-tumbling system. PThD was performed using an electric furnace with a residual field of less than 10 nT at the sample, from 100 to 680 °C. The characteristic remanent magnetization (ChRM) directions were determined based on Kirschvink's (1980) three-dimensional least squares analysis technique.

3.2. Hysteresis Properties

The hysteresis parameters of the Kawabata samples obtained from site RB16 (where stable ChRM was successfully isolated) were determined with an alternating gradient magnetometer (model MicroMag 2900, Princeton Measurements Corporation). A specimen taken from the site was gently ground in a mortar, after which 10 chips with sizes as large as 1 mm were randomly selected. After correction of the linear paramagnetic slope,

saturation magnetization (J_s), saturation remanence (J_{rs}), and coercive force (H_c) values were determined from the hysteresis loops. Together with the coercivity of remanence (H_{cr}) value obtained from backfield demagnetization procedures, these parameters were utilized to construct a correlation plot of J_{rs}/J_s versus H_{cr}/H_c (a so-called Day Plot; Day et al., 1977).

3.3. Anisotropy of Magnetic Susceptibility

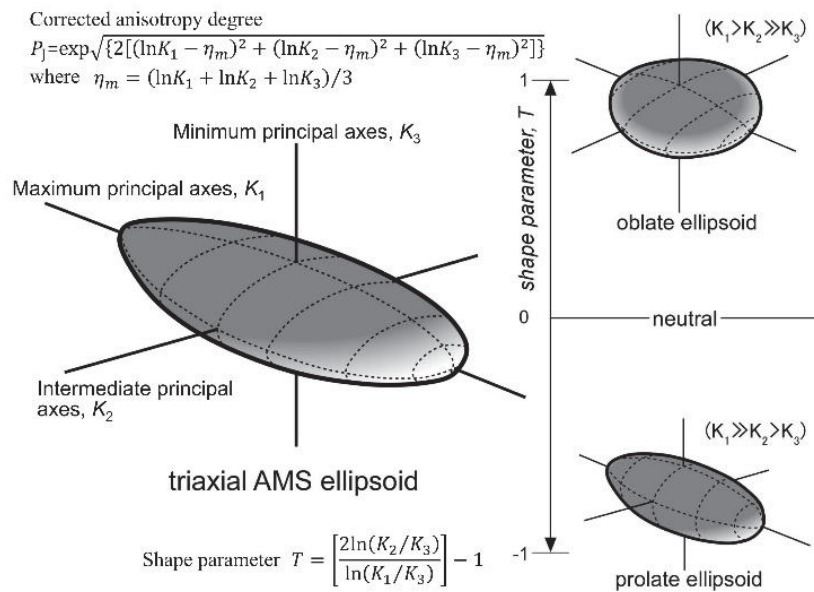


Figure 2. Schematics of susceptibility ellipsoids. Parameters related to the anisotropy of magnetic susceptibility (AMS), P_J and T , were calculated based on the orthogonal principal susceptibilities (K_1 , K_2 , K_3) as shown in the figure.

The intensity of the induced magnetization (J) is correlated with the strength of magnetic field (H) using the magnetic susceptibility (χ) of each sample, based on the relationship $J = \chi H$. The magnetic susceptibility of a rock sample is the summation of the susceptibilities of the countless mineral particles that constitute the rock. This is therefore an inherently

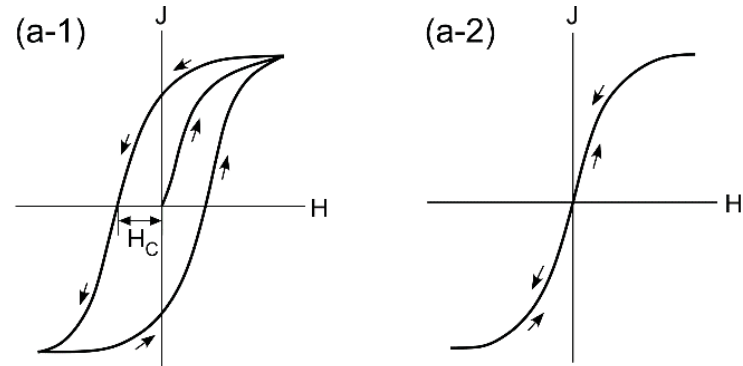
anisotropic parameter that reflects the shape magnetic anisotropy and the magnetocrystalline anisotropy of rock-forming minerals and the preferred azimuths of their alignments. Although the AMS magnitude is essentially determined by the mineral type, there is still considerable variation even in the case of a single type of mineral species, as a result of variations in physicochemical properties (Tarling and Hrouda, 1993). Figure 2 presents a schematic showing typical susceptibility ellipsoids associated with significant AMS parameters. In the present work, AMS data were acquired using an AGICO KappaBridge KLY-3 S magnetic susceptibility meter.

3.4. Magnetic Pore Fabric Assessments

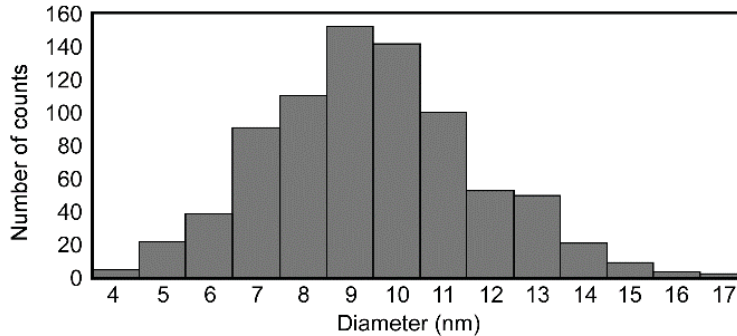
Figure 3 summarizes the general principle of magnetic analyses by means of ferrofluids. Compared to the magnetic hysteresis loops generated by a typical ferromagnetic body (Figure 3a-1), those obtained using a ferrofluid (Figure 3a-2) are characterized by negligible H_c values because the fluid contains ultrafine magnetite grains under the superparamagnetic limit (Figure 3b). Therefore, the maximum AMS axis (K_1) of a rock sample impregnated with the ferrofluid simply points to the average azimuth of the connected network of pore spaces, meaning the most permeable direction.

The ferrofluid technique was originally introduced for the purposes of oil exploration by Hailwood and colleagues (e.g., Hailwood et al., 1999) based on theoretical work by Pfeleiderer and Halls (1994). Baas et al. (2007) evaluated the use of magnetic data based on AMS as a proxy for grain orientations, and reported the advantageous measurement of a larger number of grains in a three-dimensional space in a shorter amount of time and with lower sensitivity to user bias compared to conventional microscopic observations. It should be noted that Baas et al. categorized magnetic rock inspection techniques as either enhanced AMS or Magpore, which provide information concerning the bulk grain fabric and the pore fabric, respectively (Figure 3c). Since these initial studies, researchers have attempted to apply this methodology in various fields. Nabawy et al. (2009) evaluated the correlation between the magnetic pore fabrics of an

aquifer in a sedimentary basin and the paleocurrent directions of the basin-fill, which are closely linked to the anisotropy of permeability. Almquist et al. (2011) predicted the elastic properties of porous and anisotropic synthetic materials utilizing AMS-derived pore shape geometries.



(b) Grain-size distribution



(c) Two types of AMS measurement

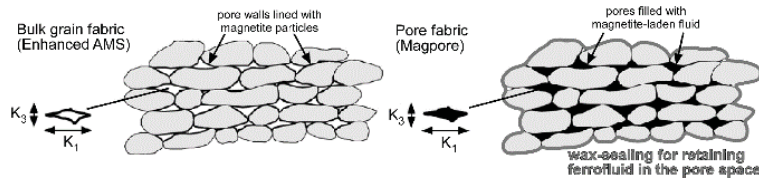


Figure 3. The physical basis of the analytical methods utilizing a suspension of a magnetic powder (that is, a ferrofluid). (a) A comparison of magnetic hysteresis curves obtained from (a-1) a conventional ferromagnetic body having a finite coercive force (H_c) and (a-2) a ferrofluid for which H_c is negligible. (b) The size distribution of the ultrafine ferrofluid particles provided by the FerroTec Co., Ltd. (c) Schematic diagrams of rock samples impregnated with ferrofluid, after Baas et al. (2007).

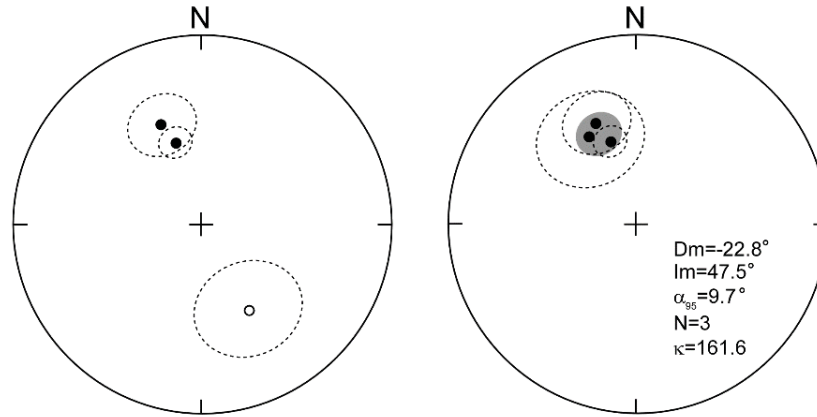
The petrophysical fundamentals of ferrofluid methodologies were recently examined by Robion et al. (2014) and Biedermann (2019). The former combined two methods based on ferrofluid impregnation and measurement of the anisotropy of acoustic velocities to obtain more reliable information concerning pores shape in porous media. The latter developed models to assist in the definition and quantification of the factors that control observable magnetic properties. AMS analyses are still regarded as a suitable means of evaluating pore fabric in place of other techniques such as optical/electron microscopy and X-ray CT. Thus, an improved theoretical understanding of such methods may allow for additional applications in geothermal, hydrological and environmental fields.

4. RESULTS: A REVIEW

4.1. Conventional Rock Magnetism

Itoh et al. (2013) previously reported that stable ChRM components were determined at three sites in the Kawabata Formation (Figure 4a). The precision parameter (κ) values for the antipodal directions were improved following tilt correction, and the formation mean direction was thought to provide a record of the Earth's dipole field. The significant westerly deflection observed in the data suggested counterclockwise rotation of the study area. It should also be noted that an opposite (clockwise) rotational motion was observed in the case of coeval sediments in central Hokkaido (Kodama et al., 1993). The contradictory results obtained from paleomagnetic studies may be attributable to differential rotations along the oblique collision front, because Tamaki et al. (2010) restored crustal deformation around the study area employed in the present work and found complicated vertical-axis rotation fields at the terminations of basin-bounding lateral faults.

(a) Kawabata Formation site-mean directions (*tilt corrected*)



(b) Sedimentological and AMS parameters

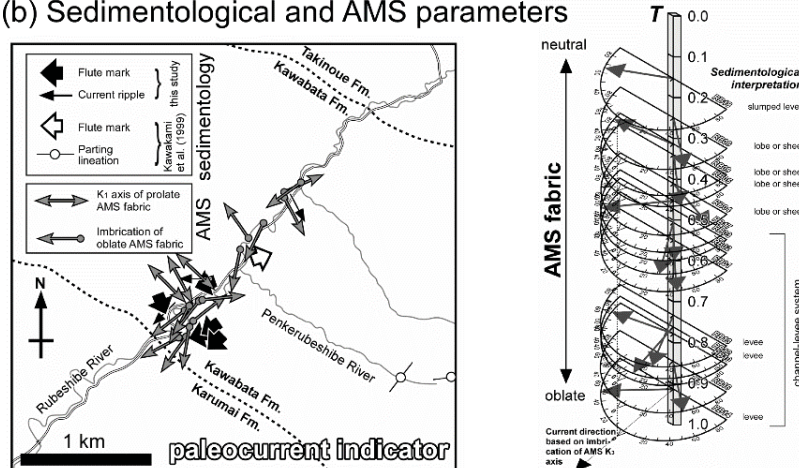


Figure 4. Conventional rock magnetic results for samples from the Kawabata Formation, after Itoh et al. (2013). (a) The site-mean ChRM directions in the study area. The solid and open circles in the equal-area projections are located on the lower and upper hemispheres, respectively, while the dotted ovals represent 95% confidence limits. The right-hand diagram has been polarity-converted to permit calculation of the formation mean direction and Fisher’s precision parameter (κ). The darkened oval is the 95% confidence limit for the formation mean. (b, left) Paleocurrent data acquired along the Rubeshibe River route. The unit boundaries are after Kawakami et al. (1999). (b, right) A summary of AMS parameters associated with paleocurrent estimation. The K_1 directions (the dark arrows) are depicted as acute angles relative to the dotted perpendicular baseline of the K_3 axis imbrication. The vertical positions of the data were determined based on T values (note that samples with negative T are not shown in this diagram).

Figure 4b (left) presents the paleocurrent indicators employed by Itoh et al. (2013). After the correction for tectonic rotation noted above, the sedimentological markers were largely indicative of a westward inflow with minor southward flow contributions, which accords with a tectono-sedimentary model of the burial process developed by Kawakami et al. (1999). As shown in the figure, the imbrication data acquired from samples with an oblate AMS fabric were found to match visible current marks. On the other hand, the K_1 axes of the prolate sites appear to be positioned at right angles to the dominant paleoflow direction, implying the rolling transportation of elongate grains on the sediment surface. Figure 4b (right) shows paleocurrent indicators determined for the Kawabata Formation as a function of the shape parameter (T) of the AMS data. The intensity of the alignment force, as inferred from the AMS values, increases on going upward along the vertical axis, which is related to the appearance of sedimentary facies (on the right side in the figure) as determined during field observations.

Figure 5a presents a typical hysteresis observed in the Kawabata Formation (RB16, comprising a muddy horizon). Here, the raw diagram suggests a minute amount of ferromagnetic minerals and Itoh et al. (2013) confirmed a weak ferromagnetic signature in this location after correction for a paramagnetic gradient. Itoh et al. also determined the hysteresis parameters for this material, as described in Section 3.2, and proposed that pseudo-single domain magnetites were the primary remanence carrier based on a correlation diagram (Day Plot). The origin of the well-grouped AMS fabric was identified using magnetic experiments with rock samples. In this procedure, the fine fraction ($< 63 \mu\text{m}$) from crushed material was processed using an isodynamic separator. After removing the ‘magnetic’ fraction (which had a high concentration of biotite), a suspension of the fine non-magnetic fraction was poured into a 1 m long plastic tube filled with water. After evaporation of water in the tube at room temperature, the artificial deposits coagulated in an adhesive resin were assessed with a magnetic susceptibility meter to determine the AMS parameters. As depicted in Figure 5b, the re-deposited Kawabata constituents comprised isotropic sediments with a negligible degree of anisotropy (P_f) and almost

zero shape parameter (T) values. These results suggest that the anisotropic nature of the natural sedimentary rocks originated from platy paramagnetic minerals such as biotite in conjunction with gravitational or hydraulic alignment forcing.

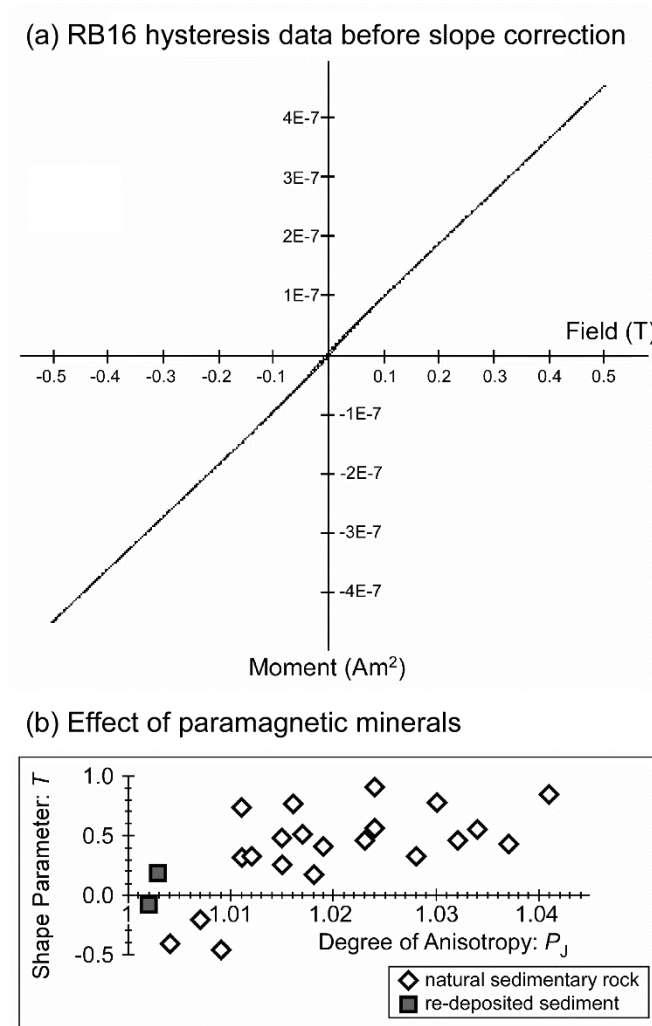


Figure 5. (a) A typical hysteresis loop for a sample from the Kawabata Formation before correction for the paramagnetic slope. (b) The AMS parameters in natural rocks and re-deposited non-magnetic fine fractions in the Kawabata Formation.

4.2. Ferrofluid Analysis

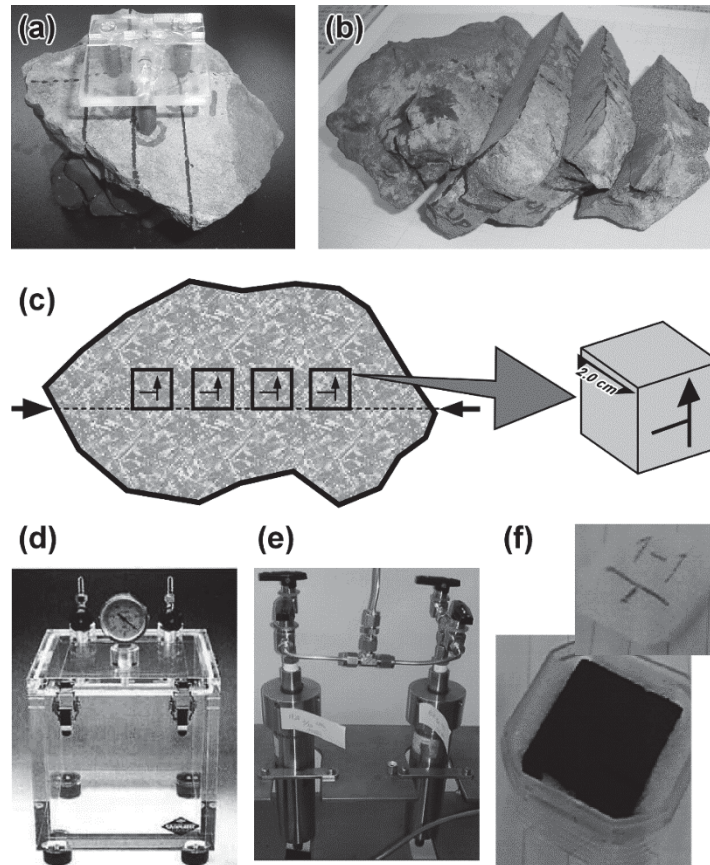


Figure 6. Sample preparation for ferrofluid experiments. (a) The marking of oriented hand samples from the RBA011 and RBA021 sites (Figure 1c). (b) The selection of rock slices free from visible cracks. (c) The shaping of cubic specimens relative to a horizontal broken line. (d) A vacuum chamber for low-pressure treatment. (e) A pressure vessel for high-pressure treatment. (f) An impregnated sample contained in a plastic capsule.

Itoh et al. (2014b) obtained samples for ferrofluid experiments, as described in Section 2, that were cut into cubic specimens each with an approximate volume of 4 cm^3 (see Figures 6a to c). In other work, Itoh et al. (2016) prepared two oriented cubes (4 cm^3 in volume) from each of 13 sites in the Kawabata Formation via the trimming of 25 mm diameter

cylindrical samples originally obtained by the same group (Itoh et al., 2013). In these studies, Itoh et al. utilized a water-based ferrofluid (MSG W10, with a saturation magnetization of 185 Gauss; manufactured by FerroTec Co., Ltd.). Itoh et al. (2014b) employed only a high-pressure method, whereas the later work (Itoh et al., 2016) treated samples using both low- and high-pressure methodologies to assess the efficiency of impregnation. Figure 6d shows the vacuum chamber employed during the low-pressure processing, in which samples were soaked in the MSG W10 fluid for 30 days. In the case of the high-pressure treatment, samples were impregnated within a pressure vessel (Figure 6e) under a pressure of 5 MPa for 30 days. Following either procedure, specimens were washed with purified water, dried and sealed in plastic capsules in preparation for the AMS measurements (Figure 6f).

Figure 7 (upper) indicates the untilted AMS fabrics of turbidite samples obtained from the Kawabata Formation. It should be noted that ferrofluid impregnation typically results in an enhancement of the degree of anisotropy in such samples. In the case of site RB01, the processed specimens (see the RBA011 figure) exhibited a prolate fabric and a significantly different spatial arrangement of principal AMS axes compared to the raw state. In contrast, specimens from the RB07 site were characterized by similar results before and after the treatment (see the RBA021 figure). The correlation between P_J and T is provided in Figure 7 (lower). Itoh et al. (2014b) attributed variations in the magnetic fabric to differences in microscale sedimentary structures. In other work, Itoh et al. (2016) performed the same analysis using samples treated with the low- and high-pressure methods and found an overall increase in the magnitude of the anisotropic fabric. They also pointed out that the low-pressure treatment did not greatly affect T , whereas the high-pressure treatment tended to reduce the T value. This means that there is a transition from oblate to prolate fabric, and it is assumed that the pressurized ferrofluid impregnated the sample via pathways that remained impermeable under atmospheric pressure, which is the same behavior as formation fluids in great depths.

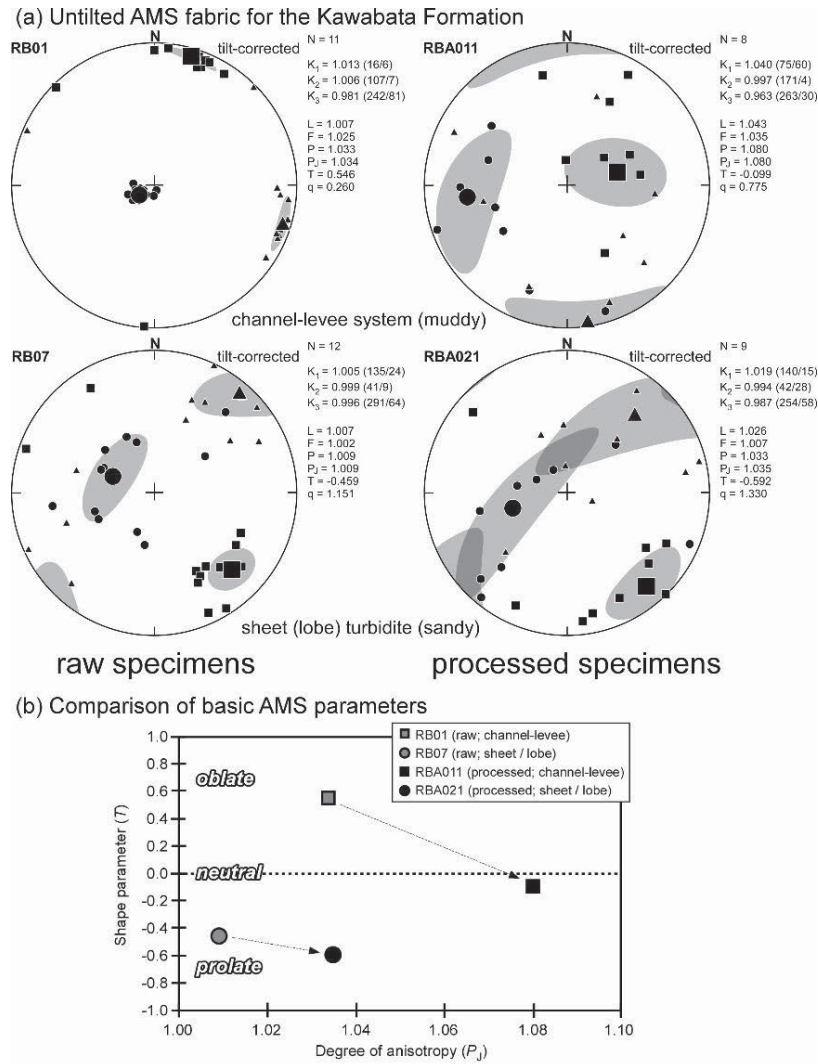


Figure 7. The effect of ferrofluid treatment on the rock magnetic properties of Kawabata samples, after Itoh et al. (2014b). (Upper) The untilted AMS fabric for the Kawabata Formation in the raw (left) and ferrofluid-soaked (right) states. All the data are on the lower hemisphere of equal-area nets. Square, triangular and circular symbols indicate the orthogonal maximum (K_1), intermediate (K_2) and minimum (K_3) AMS principal axes, respectively. Larger symbols represent mean directions and shaded areas show the 95% confidence limits based on Bingham statistics. (Lower) A comparison of the basic AMS parameters obtained for raw (RB01 and RB07) and ferrofluid-soaked (RBA011 and RBA021) samples from two sites in the Rubeshibe River route.

5. DISCUSSION

5.1. Geological Implications

A review of previous studies of rock magnetism in the Miocene Kawabata Formation in central Hokkaido confirmed the usefulness of the techniques described herein. Specifically, the remanence directions and AMS fabrics of natural rock samples can provide quantitative information concerning the tectonic and sedimentological processes in the Kawabata basin. The anisotropic parameters of the ferrofluid-impregnated samples also increase our understanding of the cause and effect relationship between regional tectonic events and the development of microscopic fractures in rocks. As an example, the permeable directions indicated by the principal AMS axes are enhanced under high pressure (Figure 7, upper right) and evidently lie in the plane of a basin-bounding reverse fault activated by intensive stress around the oblique collision front. Two techniques are required to verify this interpretation. First, it is important to assess the experimental conditions using a large number of test specimens. Our analyses indicate that the impregnation efficiency is affected by the lithofacies of the samples (Itoh et al., 2016). Parés et al. (2016) evaluated the usability of water- and oil-based ferrofluids, and their work is also important from the second viewpoint, establishing the origin of the fabric. Parés et al. examined the origin of micro-porosity based on close observations of clay fabrics. Similarly, Itoh et al. (2016) employed micro-focus X-ray CT scanning for the three-dimensional visualization of fracture networks, and obtained a number of unexpected findings, as described in Section 5.2.

5.2. Impact on Paleontological Studies

In an effort to precisely evaluate the effect of ferrofluid penetration, Itoh et al. (2016) obtained a series of X-ray CT images of impregnated Kawabata samples using an HMX225-ACTIS+3 Micro-Focus X-Ray CT

Scanner at Center for Advanced Marine Core Research, Kochi University. As depicted in Figure 8a, they acquired 601 images per sample with a spatial resolution of 30 μm . These images indicated that the penetration efficiency varied even at the same site as a result of microscopic structural disturbances, some of which originated from bioturbation delineated by sinuous paths which the dense fluid followed (Figure 8b). The authors observed fine biogenic structures by employing an OsiriX MD DICOM viewer that enabled semi-stereographic visualization by stacking many half-transparent images (Figure 8c-1). Amazingly, these observations showed both trace fossils and fragments of living organisms having internal structures (Figure 8c-2). However, higher imaging resolution is inevitably required for more detailed analysis of such exquisite objects.

When a rock sample is infused with the ferrofluid and observed via X-ray CT scan imaging, the resulting images are not of uniform brightness, but rather exhibit a mosaic of lighter and darker regions reflecting the nonuniform extent of slurry penetration. If a number of such images are superposed and converted to volumetric data, the resulting data set contains information encoded in the spatial distribution of brightness values. By defining certain threshold brightness values and successively visualizing the corresponding constant-brightness surfaces, we have successfully extracted three-dimensional images (Figure 8d-1), which we are able to observe and record from arbitrary angles, representing the distribution of microfossils embedded in the sample. The example fossil in Figure 8d-2 and 3 is captured from the same region of interest as that in Figure 8c-2.

Previous research in this field involved efforts to reconstruct the morphologies of small fossils; one particularly well-known example is the study of the Burgess Shale in the Canadian Rocky Mountains, which shed light on the nature of the Cambrian explosion. The extraction procedure used in this study involved the use of a drill to remove thin films of biological tissue, layered parallel to the sedimentary layers of the strata, which were then sketched and accumulated. An unfortunate consequence was that precious fossils were lost entirely along with their descriptions.

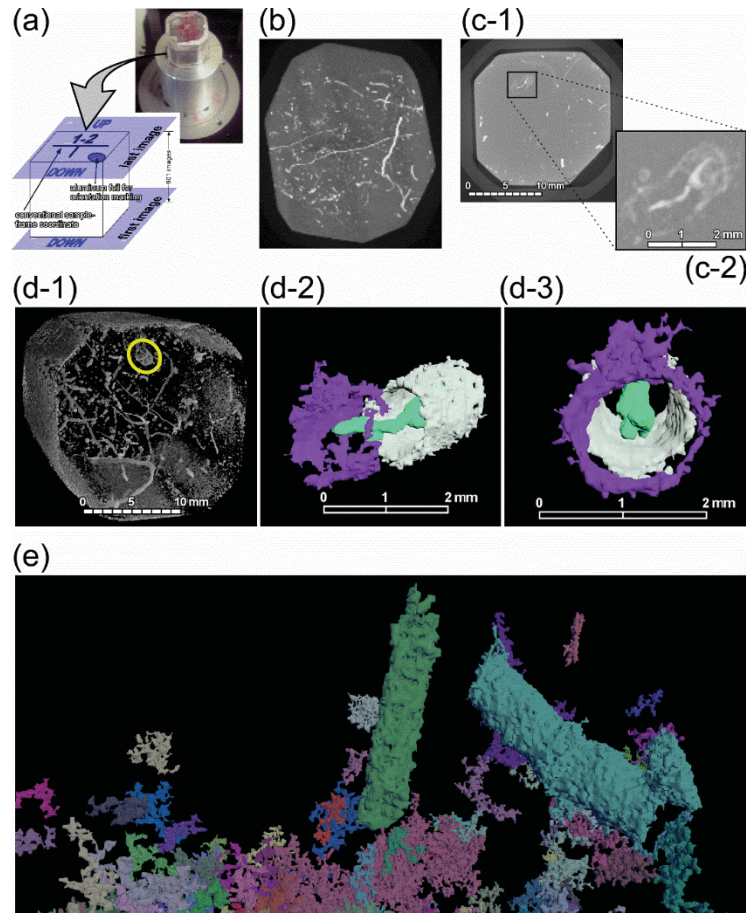


Figure 8. Digital images acquired from X-ray CT scanning data for rock samples taken from the Kawabata Formation after impregnation with ferrofluid. (a) The rule of sample orientation for acquiring 601 sequential tomographic images. (b) A three-dimensional maximum intensity projection image of the ferrofluid-processed specimen RB0371 as generated by the OsiriX MD software. (c-1) A two-dimensional thick slab view (from the stacking of 67 images) of the ferrofluid-processed specimen RB0371 as generated by the OsiriX MD. (c-2) A close-up of a microfossil found in the two-dimensional thick slab image. (d-1) The extracted three-dimensional image of constant-brightness surfaces obtained from volumetric data which were converted from an X-ray CT sequence of the ferrofluid-processed specimen RB0371. (d-2) A close-up (side view) of a microfossil in the yellow enclosure found in the extracted three-dimensional image. (d-3) A close-up (front view) of a microfossil in the yellow enclosure found in the extracted three-dimensional image. (e) Numerous microfossils as visualized by the digital imaging technology.

The revolutionary advantage of our new technique is its ability to acquire morphology data non-destructively. Moreover, despite the intense diagenetic effects that accompany the burial process, fossils preserved in turbidite samples exhibit only slight deformation due to nonuniform pressure fields (their shapes are not particularly planar), and the ability of our method to yield undistorted three-dimensional images of any arbitrary sample of interest, without the need for a lengthy, complex process of morphology reconstruction, is perhaps the most noteworthy aspect of the present work. Although the observation of biofacies in marine sediments is essential for the reconstruction of oceanic paleoenvironments (e.g., Arthur and Sageman, 1994), such examinations are often biased by variations in fossil preservation and the inability to perform quantitative evaluations. Our fine visualization technique (see Figure 8e) may allow a more comprehensive understanding of epoch-making events in the Earth's history, such as recurrent mass extinctions.

CONCLUSION

A wide range of rock magnetic analyses was performed using samples from an event sedimentary sequence in central Hokkaido (the Miocene Kawabata Formation) to assess the properties of turbidite units. The following conclusions can be made.

1. The untilted stable ChRM directions of the Kawabata Formation are suggestive of counterclockwise rotation around the study area since the Miocene, which in turn is related to differential rotations along the oblique collision front.
2. The AMS fabrics of natural rock samples provide quantitative information regarding the sedimentological processes in the Kawabata basin. The sedimentological markers, after correction for tectonic tilt and rotation, are largely indicative of a westward inflow with minor southward flow components, which accords with a tectono-sedimentary model for the burial process.

3. The AMS parameters of the ferrofluid-impregnated Kawabata samples assist in understanding the causal relationship between regional tectonics and the formation of microscopic fractures in rocks. The pressurized ferrofluid evidently impregnated the samples via specific pathways that were originally produced during intensive collision events and remained impermeable under atmospheric pressure.
4. Micro-focus three-dimensional density images of ferrofluid-laden samples are obtained utilizing an X-ray CT scanner and high-resolution digital image processing techniques. This process can successfully depict the morphologies of small fossils to allow detailed analysis of paleoenvironmental conditions. Attractive movies of the reconstructed microorganisms are available at OPERA: Osaka Prefecture University Education and Research Archives (<http://hdl.handle.net/10466/00016749>).

ACKNOWLEDGMENTS

The authors are grateful to Nobuhiko Hayashi, Takayuki Yoshida and Tsubasa Hasegawa for their support during the digital imaging of computerized tomography data at NHK Art, Inc.

REFERENCES

- Almqvist, B.S.G., Mainprice, D., Madonna, C., Burlini, L., & Hirt, A.M. (2011). Application of differential effective medium, magnetic pore fabric analysis, and X-ray microtomography to calculate elastic properties of porous and anisotropic rock aggregates. *Journal of Geophysical Research*, 116, B01204, doi:10.1029/2010JB007750.

- Arthur, M.A., & Sageman, B.B. (1994). Marine black shales: depositional mechanisms and environments of ancient deposits. *Annual Review of the Earth and Planetary Sciences*, 22, 499-551.
- Baas, J.H., Hailwood, E.A., McCaffrey, W.D., Kay, M., & Jones, R. (2007). Directional petrological characterisation of deep-marine sandstones using grain fabric and permeability anisotropy: methodologies, theory, application and suggestions for integration. *Earth-Science Reviews*, 82, 101-142.
- Biedermann, A.R. (2019). Magnetic pore fabrics: the role of shape and distribution anisotropy in defining the magnetic anisotropy of ferrofluid-impregnated samples. *Geochemistry, Geophysics, Geosystems*, doi:10.1029/2019GC008563.
- Day, R., Fuller, M., & Schmidt, V.A. (1977). Hysteresis properties of titanomagnetites: grain-size and compositional dependence. *Physics of Earth and Planetary Interiors*, 13, 260-267.
- Hailwood, E.A., Bowen, D., Ding, F., Corbett, P.W.M., & Whattler, P. (1999). Characterizing pore fabrics in sediments by anisotropy of magnetic susceptibility analyses. In D.H. Tarling and P. Turner (Eds.), *Palaeomagnetism and Diagenesis in Sediments*. Geological Society, London, Special Publications, 151, 125-126.
- Itoh, Y., Tamaki, M., & Takano, O. (2013). Rock magnetic properties of sedimentary rocks in central Hokkaido - insights into sedimentary and tectonic processes on an active margin. In Y. Itoh (Ed.), *Mechanism of Sedimentary Basin Formation - Multidisciplinary Approach on Active Plate Margins*. Rijeka (Croatia): InTech. <http://dx.doi.org/10.5772/56650>.
- Itoh, Y., Takano, O., Kusumoto, S., & Tamaki, M. (2014a). Mechanism of long-standing Cenozoic basin formation in central Hokkaido: an integrated basin study on an oblique convergent margin. *Progress in Earth and Planetary Science*, 1:6. doi:10.1186/2197-4284-1-6.
- Itoh, Y., Takano, O., & Tamaki, M. (2014b). Quantitative analysis of pore network in rocks utilizing ferrofluids: application of rock magnetic data for oil exploration. *Journal of the Japanese Association for Petroleum Technology*, 79, 339-348.

- Itoh, Y., Takano, O., & Tamaki, M. (2016). Evaluation of micro-fabric network within marine sediments based on a rock magnetic technique. In S. Williams (Ed.), *Marine Sediments*. New York: Nova Science Publishers, Inc., 43-59.
- Itoh, Y., Takano, O., & Takashima, R. (2017). Tectonic synthesis: a plate reconstruction model of the NW Pacific region since 100 Ma. In Y. Itoh (Ed.), *Dynamics of Arc Migration and Amalgamation - Architectural Examples from the NW Pacific Margin*. Rijeka (Croatia): InTech. <http://dx.doi.org/10.5772/67358>.
- Kawakami, G. (2013). Foreland basins at the Miocene arc-arc junction, central Hokkaido, northern Japan. In Y. Itoh (Ed.), *Mechanism of Sedimentary Basin Formation - Multidisciplinary Approach on Active Plate Margins*. Rijeka (Croatia): InTech. <http://dx.doi.org/10.5772/56748>.
- Kawakami, G., Yoshida, K., & Usuki, T. (1999). Preliminary study for the Middle Miocene Kawabata Formation, Hobetsu district, central Hokkaido, Japan: special reference to the sedimentary system and the provenance. *Journal of the Geological Society of Japan*, 105, 673-686.
- Kirschvink, J.L. (1980). The least-squares line and plane and the analysis of palaeomagnetic data. *Geophysical Journal of the Royal Astronomical Society*, 62, 699-718.
- Kodama, K., Takeuchi, T., & Ozawa, T. (1993). Clockwise tectonic rotation of Tertiary sedimentary basins in central Hokkaido, northern Japan. *Geology*, 21, 431-434.
- Nabawy, B.S., Rochette, P., & Geraud, Y. (2009). Petrophysical and magnetic pore network anisotropy of some Cretaceous sandstone from Tushka Basin, Egypt. *Geophysical Journal International*, 177, 43-61.
- Otofujii, Y., Kambara, A., Matsuda, T., & Nohda, S. (1994). Counterclockwise rotation of northeast Japan: paleomagnetic evidence for regional extent and timing of rotation. *Earth and Planetary Science Letters*, 121, 503-518.
- Parés, J.M., Miguens, L., & Saiz, C. (2016). Characterizing pore fabric in sandstones with magnetic anisotropy methods: initial results. *Journal*

- of Petroleum Science and Engineering*, 143, 113-120, <http://dx.doi.org/10.1016/j.petrol.2016.02.028>.
- Pfleiderer, S., & Halls, H.C. (1994). Magnetic pore fabric analysis: a rapid method for estimating permeability anisotropy. *Geophysical Journal International*, 116, 39-45.
- Robion, P., David, C., Dautriat, J., Colombier, J-C., Zinsmeister, L., & Collin, P-Y. (2014). Pore fabric geometry inferred from magnetic and acoustic anisotropies in rocks with various mineralogy, permeability and porosity. *Tectonophysics*, 629, 109-122, <http://dx.doi.org/10.1016/j.tecto.2014.03.029>.
- Tamaki, M., Kusumoto, S., & Itoh, Y. (2010). Formation and deformation processes of late Paleogene sedimentary basins in southern central Hokkaido, Japan: paleomagnetic and numerical modeling approach. *Island Arc*, 19, 243-258.
- Tarling, D.H., & Hrouda, F. (1993). *The Magnetic Anisotropy of Rocks*. London: Chapman & Hall, 217pp.